

Fluorocitrate Inhibition of Aconitase: Relative Configuration of Inhibitory Isomer by X-ray Crystallography

Abstract. *The fluorocitrate isomer that is a strong inhibitor and inactivator of aconitase has been shown by x-ray crystallographic studies on the rubidium ammonium salt to have the configurations (1R:2R) or (1S:2S) 1-fluoro-2-hydroxy-1,2,3-propanetricarboxylic acid. A possible mechanism for the action of fluorocitrate is proposed which involves the 1R:2R isomer suggested from biochemical data.*

Extensive studies by Peters and his collaborators (1) showed that the toxicity of fluoroacetate in animals is due to its enzymatic conversion to fluorocitrate, which then acts as an inhibitor of aconitase [E.C. 4.2.1.3, citrate (isocitrate) hydro-lyase]. Further examination of this mechanism reveals that the mode of interaction of aconitase with fluorocitrate consists of an initial, apparently competitive inhibition of the enzyme by fluorocitrate, followed by a time-dependent inactivation of aconitase (2). This second type of interaction, the inactivation, can occur at very low concentrations of the inhibitor. It was also shown that succinic dehydrogenase is inhibited by

fluorocitrate, but this inhibition is not as powerful as that of aconitase (1, 3). The molecular mechanism of the inactivation of aconitase by fluorocitrate was assumed (3) to be the result of alkylation of the enzyme at its active site. This type of inactivation would be expected to depend on a stereospecific interaction between the inhibitory isomer of fluorocitrate and the active site, which contains ferrous iron, and which has been depicted by Glusker (4).

It was shown that the inhibitory isomer of fluorocitrate is formed by the enzymatically catalyzed condensation of fluoroacetyl coenzyme A and oxalacetate, but that the fluorocitrate

derived from fluoroacetyl coenzyme A was not inhibitory (2). However, these two enzymatically synthesized fluorocitrates are enantiomorphs. The chemical synthesis of all four isomers of fluorocitrate and their resolution (5, 6) made possible a more detailed study of the stereospecificity of aconitase inhibition by fluorocitrate. We now report an x-ray crystallographic analysis of the racemic modification of fluorocitrate which contains the inhibitory species.

The rubidium ammonium salt of the racemate of the diastereoisomer of fluorocitric acid that contains the active inhibitor of aconitase was prepared chemically (5). The salt formed triclinic crystals with cell dimensions $a = 8.458$, $b = 10.910$, $c = 7.517$ Å, $\alpha = 102.8^\circ$, $\beta = 115.9^\circ$, $\gamma = 80.5^\circ$; $V = 600.1$ Å³. The density, measured by flotation in a mixture of *m*-xylene and bromoform, is 1.92 g cm⁻³, that calculated for two units of $[\text{Rb}(\text{NH}_4)(\text{C}_6\text{H}_5\text{O}_7\text{F})] \cdot 2\text{H}_2\text{O}$ is 1.925 g cm⁻³.

The crystal chosen for the data collection had the dimensions of 0.15 mm on an edge. Data were collected with nickel-filtered copper x-radiation by the stationary-crystal stationary-counter technique on a Picker automatic diffractometer (at the Laboratory for Research on the Structure of Matter, University of Pennsylvania, Philadelphia). This method of data collection was used because the crystal, even when coated, deteriorated with time. All data up to $2\theta = 130^\circ$ were measured. The space group was determined to be $P\bar{1}$ because no anomalous dispersion effects were observed, implying that this is a centric structure. Differences in intensity measured for equivalent reflections (hkl and $\bar{h}\bar{k}\bar{l}$) were within 4 standard deviations for the individual intensities. Lorentz, polarization, and absorption corrections were made.

The structure was solved from the Patterson map and refined by the method of block diagonal least squares to an R value of 0.059. There is some disorder in the crystal that involves the cations which are almost identical in size, that is, the "rubidium" ion is best represented as 85 percent rubidium and 15 percent ammonium, and the reverse is true for the "ammonium" ion. This type of disorder has already been noted in rubidium ammonium citrate (7).

The analysis (8) has shown that the isomers in this racemic crystal have the 1R:2R and 1S:2S configurations (9)

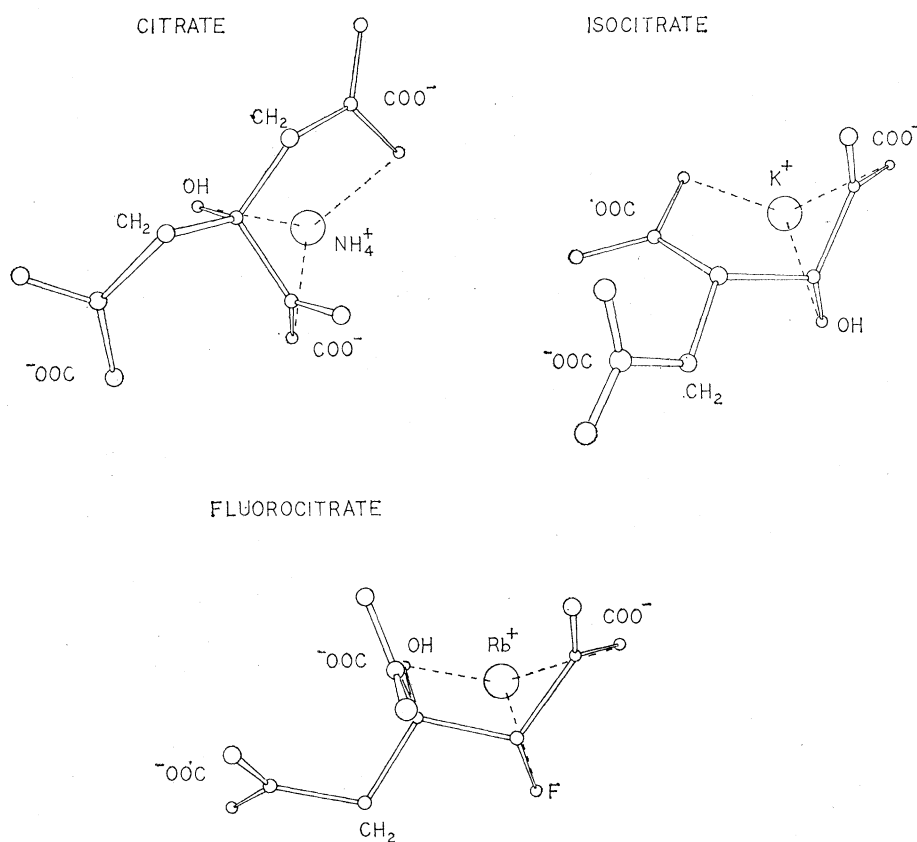
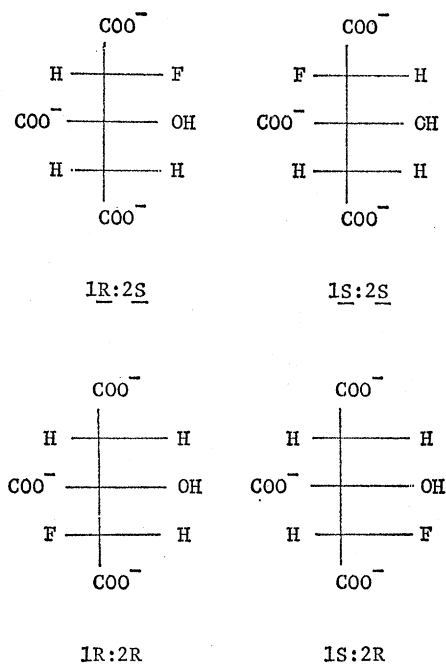


Fig. 1. A comparison of the crystallographically determined conformations of metal chelates of citrate (lithium ammonium hydrogen citrate monohydrate) and isocitrate (potassium dihydrogen isocitrate) with the chelate of the active isomer of fluorocitrate.

for 1-fluoro-2-hydroxy-1,2,3-propanetricarboxylic acid as shown below:



The x-ray analysis has also shown that the ion forms a tridentate chelate to the rubidium ion through the fluorine atom, the oxygen atom of the hydroxyl group, and the oxygen atom of the terminal carboxyl group adjacent to the -CHF-group.

Since it is difficult to differentiate fluorine from oxygen by x-ray crystallographic techniques because the hydroxyl group is isoelectronic with the fluorine atom, the nature of this atom was checked further in order to ascertain that hydrolysis of the C-F bond had not occurred and that a hydroxycitrate had not been studied. The environment of the atom under investigation showed no evidence of hydrogen bonding, which could be expected of a hydroxyl group, but the interatomic distances found and the peak counts did not resolve this question of identity with certainty. Therefore the proton nuclear magnetic resonance spectrum of a solution of the crystals in D_2O was measured on a Varian 100 Mhz instrument at 75°C . The spectrum contained a -CHF- doublet with a coupling constant $J = 48$ hz as found for esters of fluorocitric acid in deuteriochloroform (2). The difference in chemical shift between the center of the -CHF- doublet and the -CH₂- peak was found to be 2.24 ppm compared with values of 2.05 and 2.15 for the esters of the two isomers reported in the reference above. These results

demonstrate unequivocally that a fluoro-citrate and not a hydroxycitrate has been studied.

Enzymatic studies on the salt were made with purified aconitase (10) from pig heart cytoplasm. The fluoro-citrate salt is a linear competitive inhibitor with respect to citrate (Michaelis constant $K_m = 6.2 \times 10^{-4}M$) with an inhibition constant K_i value of $2.9 \times 10^{-4}M$ for the racemic mixture. An assay in which the rate of formation of isocitrate is monitored (11) was used. This K_i value is higher than the value of 10^{-6} reported for the enzyme from rat liver mitochondria (3). On prolonged incubation the salt inactivated the cytoplasmic enzyme, as has been described for the mitochondrial enzyme (3).

The inhibitory isomer of fluorocitrate is formed in vivo from fluoroacetate by the reaction catalyzed by citrate synthase (E.C. 4.1.3.7). This enzyme, extracted from pig heart, introduces the acetate group into the *pro-S* position of citrate (12). This is the position which, on replacement of fluorine by hydrogen, would be in the lower half of each of the formulas for fluoro-citrate illustrated above. Therefore, if we assume the same absolute stereo-

chemistry for the citrate synthase reaction with fluoroacetyl coenzyme A as with acetyl coenzyme A, the active isomer must have a fluorine atom in the lower half of the formulas above, that is, it has one of the 2R configurations. The crystallographic studies demonstrated the 1R:2R and the 1S:2S configurations for the racemate. Thus it is concluded, with the above assumption on the action of citrate synthase, that the inhibitory isomer has the 1R:2R configuration. Crystallographic studies have now been initiated on a cyclohexylamine fluorocitrate in order to determine the absolute configuration of the inhibitory isomer.

The nature of the inhibition may now be considered in detail. It has been found from an analysis of the crystallographic results and from model building that only the inhibitory (1R:2R) isomer of fluorocitrate can fit in the active site in a manner similar to that proposed for citrate or isocitrate in an enzyme-ferrous-substrate ternary complex (4). This is illustrated in Fig. 1 in which a comparison of the crystallographically determined conformations of the metal chelates of citrate, isocitrate, and the fluorocitrate is made.

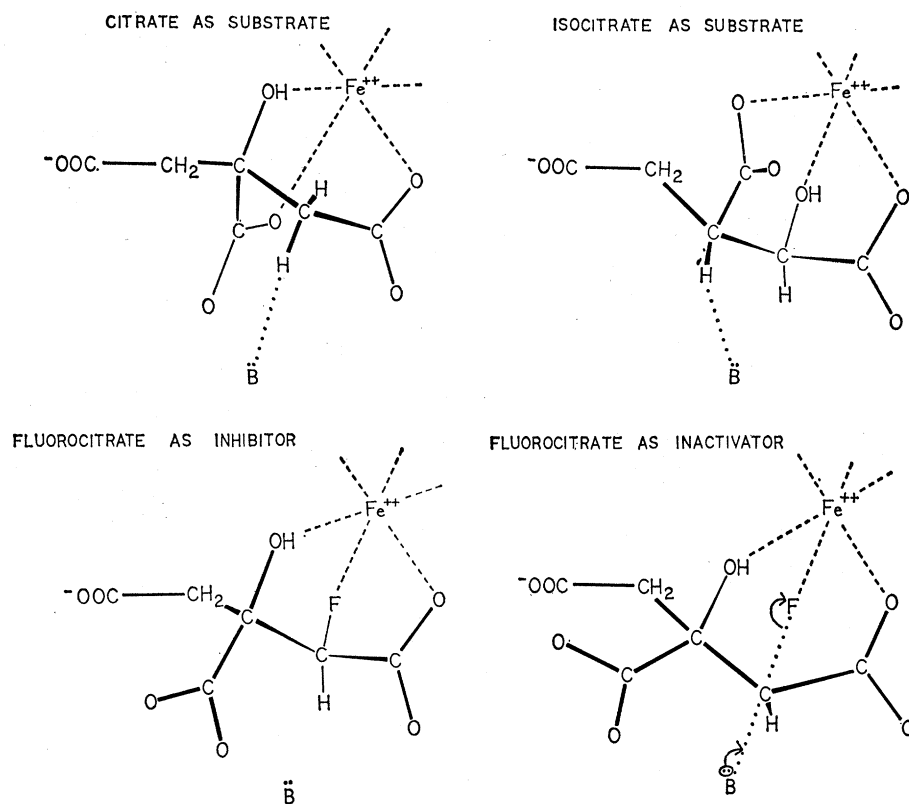


Fig. 2. The proposed mechanism of inhibition and inactivation of aconitase by fluorocitrate.

Tritium exchange reactions catalyzed by aconitase have shown the involvement of a basic proton-abstracting group on the enzyme (11). Coordination of the fluorine of fluorocitrate to the enzyme-bound metal could facilitate the substitution of fluoride by the proton-abstracting group of the enzyme and lead to irreversible inhibition. The spatial arrangements of the fluorine and the proton-abstracting group are illustrated in Fig. 2. Thus, the crystallographic model explains both the competitive inhibition and the slower inactivation of aconitase by fluorocitrate.

H. L. CARRELL, JENNY P. GLUSKER
J. J. VILLAFRANCA, A. S. MILDVAN
*The Institute for Cancer Research,
Philadelphia, Pennsylvania 19111*

R. J. DUMMEL, E. KUN
*Department of Pharmacology and
Cardiovascular Research Institute,
University of California, School of
Medicine, San Francisco*

References and Notes

1. F. L. M. Pattison and R. A. Peters, in *Handbook of Experimental Pharmacology* (Springer, New York, 1966), vol. 20, chap. 8, pp. 387-458.
2. D. W. Fanshier, L. K. Gottwald, E. Kun, *J. Biol. Chem.* **239**, 425 (1964).
3. E. Kun, in *Citric Acid Cycle. Control and Compartmentation*, J. M. Lowenstein, Ed. (Dekker, New York, 1969), chap. 6, p. 318.
4. J. P. Glusker, *J. Mol. Biol.* **38**, 149 (1968).
5. R. J. Dummel and E. Kun, *J. Biol. Chem.* **244**, 2966 (1969).
6. K. Kirk and P. Goldman, *Biochem. J.* **117**, 409 (1970).
7. W. E. Love and A. L. Patterson, *Acta Cryst.* **13**, 426 (1960).
8. H. L. Carrell and J. P. Glusker, full details are being prepared for publication.
9. R. S. Cahn, C. Ingold, V. Prelog, *Angew. Chem. Int. Ed.* **5**, 385 (1966).
10. J. J. Villafranca and A. S. Mildvan, *J. Biol. Chem.*, in press.
11. I. A. Rose and E. L. O'Connell, *ibid.* **242**, 1870 (1967).
12. K. R. Hanson and I. A. Rose, *Proc. Nat. Acad. Sci. U.S.A.* **50**, 981 (1963); H. Eggerer, W. Buckel, H. Lenz, P. Wunderwald, G. Gottschalk, J. W. Cornforth, C. Donninger, R. Mallaby, J. W. Redmond, *Nature* **226**, 517 (1970); J. Rétey, J. Lüthy, D. Arigoni, *ibid.*, p. 519.
13. We thank C. A. Casciato and J. Dargay for technical assistance and Professor Jerry Donohue for the use of the automatic diffractometer at the University of Pennsylvania, Philadelphia. Supported by NIH grants CA-10925, CA-06927, RR-05539, AM-13351, and HD-01239; NSF grant GB-8579; American Cancer Society grant E-493; and by an appropriation from the Commonwealth of Pennsylvania. J.J.V. is an NIH postdoctoral fellow 1-F02-AM-42758-01, A.S.M. is an Established Investigator of the American Heart Association, and E.K. is a Research Career Awardee of the PHS.

26 August 1970; revised 8 October 1970

Threonine Deaminase: A Novel Activity Stain on Polyacrylamide Gels

Abstract. *With phenazine methosulfate and nitro blue tetrazolium, an activity stain for threonine deaminase has been developed. Because the deamination reaction does not involve any overall oxidation or reduction, it is proposed that one of the intermediates of the reaction, α -aminocrotonate or α -iminobutyrate, is the reducing agent. Studies with ferricyanide as the artificial electron acceptor indicate that a decarboxylation of the intermediate occurs during the dye reduction.*

The ability to identify a protein band with a specific enzyme activity by an activity stain in situ after electrophoresis on polyacrylamide or starch gels has proven useful in exploring a variety of

questions. For example, with such a stain, the existence of isoenzymes can be established, even in relatively crude extracts. Similarly, this simple technique can provide valuable information about

Table 1. Production of CO_2 during ferricyanide reduction. Reaction mixtures were placed in Thunberg tubes, with the side arm containing 0.4 ml of 0.1N KOH. The first reaction mixture contained 100 μmole of potassium phosphate buffer (pH 8), 20 μmole of L-threonine, 0.5 μC uniformly labeled [^{14}C]threonine (130 mc/mmole), and enzyme in a volume of 1.0 ml. In addition, the second reaction mixture contained 2.5 μmole of potassium ferricyanide. The reaction was initiated by adding 40 μg of enzyme to each mixture. After incubation for 5 minutes at 25°C, the reactions were stopped by adding 0.5 ml of a 1:1 mixture of 30 percent trichloroacetic acid and 0.2 percent dinitrophenylhydrazine in 2.0N HCl, thus trapping α -keto-butyrate formed as the hydrazone derivative to prevent any acid-catalyzed decarboxylation of the keto acid. After further incubation for 30 minutes at 25°C, 0.2 ml of KOH from the side arm was pipetted onto an etched glass disk along with 0.2 ml of 0.1M BaCl_2 in 50 percent ethanol. The disks were dried and counted on a gas-flow planchet counter. In calculating the actual CO_2 generated, an efficiency of 25 percent was used to convert counts per minute to disintegrations per minute (dpm). Under identical assay conditions with nonradioactive threonine as substrate, 0.47 μmole of ferrocyanide was produced in 5 minutes, as measured spectrophotometrically.

Reaction mixture	$^{14}\text{CO}_2$ in 0.4 ml of KOH (dpm)	Total $^{14}\text{CO}_2$ (μmole)	μmole ferricyanide reduced/ μmole $^{14}\text{CO}_2$ produced
No ferricyanide	240	0.02	
Ferricyanide	6592	0.49	0.96

changes in protein structure or association-dissociation behavior of enzymes in the presence or absence of ligands. Unfortunately, activity stains in situ have been developed for only a few enzymes. The most familiar activity stain is that for the various dehydrogenases (1) where pyridine nucleotide or flavin nucleotide coenzymes participate in the enzyme-catalyzed oxidation of substrates. In addition to the dehydrogenases, activity stains have been developed for polynucleotide phosphorylase (2), alkaline phosphatase (3), esterases (4), and several other enzymes (4).

To stain for dehydrogenase activity after electrophoresis, the gel is incubated in a buffered solution containing the oxidized coenzyme and the reduced substrate in the presence of phenazine methosulfate (PMS) and nitro blue tetrazolium (NBT). The oxidation of the substrate in the enzyme-catalyzed reaction reduces the coenzyme which, in turn, reduces the PMS. Finally, the reduced PMS is reoxidized with concomitant reduction of NBT. In the oxidized state, NBT is soluble and colorless, while in the reduced form it is insoluble and has a purple color. Hence, a purple precipitant band is visible on the gel coincident with the site of dehydrogenase activity.

In the search for an activity stain for L-threonine deaminase [L-threonine hydrolyase (deaminating) (E.C. 4.2.1.-16)] from *Rhodospirillum rubrum*, we found that the combination of PMS and NBT in the presence of threonine also generated a purple precipitant band. Threonine deaminase, purified to homogeneity (5), was subjected to electrophoresis on polyacrylamide gels (Fig. 1). Gel 2 (Fig. 1A) was stained for protein with amido black, whereas gels 1 and 3 were stained for enzyme activity with L-threonine and L-serine as substrate, respectively (6). The two bands in gel 2, corresponding to the native enzyme and a dimer of the native enzyme (5), were both active with either substrate. Partially purified enzyme preparations displayed a large number of protein bands, but when stained for enzyme activity showed only two bands in the same relative positions as those seen in Fig. 1A. The control experiments (Fig. 1B) demonstrated that omission of substrate, PMS, or NBT resulted in no purple precipitant band.

To demonstrate that the threonine deaminase was indeed located in those regions showing precipitant bands, puri-